Available online at www.sciencedirect.com
SCIENCE DIRECT®
Ocean Modelling 8 (2005) 1–30
Ocean Modelling
www.elsevier.com/locate/ocemod

Modeling mesoscale eddies

V.M. Canuto [a,b,*], M.S. Dubovikov [a,c]

[a] Goddard Institute for Spaces Studies, NASA, 2880 Broadway, New York, NY 10025, USA
[b] Department of Applied Physics and Mathematics, Columbia University, New York, NY 10027, USA
[c] Center for Climate System Research, Columbia University, New York, NY 10025, USA

Received 16 July 2003; received in revised form 8 October 2003; accepted 24 November 2003
Available online 6 December 2003

Abstract

Mesoscale eddies are not resolved in coarse resolution ocean models and must be modeled. They affect both mean momentum and scalars. At present, no generally accepted model exists for the former; in the latter case, mesoscales are modeled with a bolus velocity $\mathbf{u}_*$ to represent a sink of mean potential energy. However, comparison of $\mathbf{u}_*$(model) vs. $\mathbf{u}_*$ (eddy resolving code, [J. Phys. Ocean. 29 (1999) 2442]) has shown that $\mathbf{u}_*$(model) is incomplete and that *additional terms*, ''unrelated to thickness source or sinks'', are required. Thus far, no form of the additional terms has been suggested.

To describe mesoscale eddies, we employ the Navier–Stokes and scalar equations and a turbulence model to treat the non-linear interactions. We then show that the problem reduces to an eigenvalue problem for the mesoscale Bernoulli potential. The solution, which we derive in analytic form, is used to construct the momentum and thickness fluxes. In the latter case, the bolus velocity $\mathbf{u}_*$ is found to contain two types of terms: the first type entails the gradient of the mean potential vorticity and represents a positive contribution to the production of mesoscale potential energy; the second type of terms, which is new, entails the velocity of the mean flow and represents a negative contribution to the production of mesoscale potential energy, or equivalently, a backscatter process whereby a fraction of the mesoscale potential energy is returned to the original reservoir of mean potential energy. This type of terms satisfies the physical description of the additional terms given by [J. Phys. Ocean. 29 (1999) 2442].

The mesoscale flux that enters the momentum equations is also contributed by two types of terms of the same physical nature as those entering the thickness flux. The potential vorticity flux is also shown to contain two types of terms: the first is of the gradient-type while the other terms entail the velocity of the mean flow. An expression is derived for the mesoscale diffusivity κ_M and for the mesoscale kinetic energy K

* Corresponding author. Address: Goddard Institute for Spaces Studies, NASA, 2880 Broadway, New York, NY 10025, USA. Tel.: +1-212-6785571; fax: +1-212-6785560.
E-mail address: vcanuto@giss.nasa.gov (V.M. Canuto).

1463-5003/$ - see front matter
doi:10.1016/j.ocemod.2003.11.003

in terms of the large-scale fields. The predicted $\kappa_M(z)$ agrees with that of heuristic models. The complete mesoscale model in isopycnal coordinates is presented in Appendix D and can be used in coarse resolution ocean global circulation models.

1. The problem

Coarse resolution ocean codes (e.g., those used in climate studies, Griffies et al., 2000) can only resolve the largest structures and leave the mesoscale eddies (50–100) km to be modeled. To separate the resolved from the unresolved scales, one first averages the equations for the momentum and thickness. The averaging for the momentum equations is not unique, as Greatbatch (2001) and Greatbatch and McDougall (2003) have recently discussed in detail. The key point, however, is that while some representations may highlight some physical features more clearly than others (e.g., how eddies influence the mean flow, Wardle and Marshall, 2000), they always require an additional input, *a model to express the contribution of the unresolved scales in terms of the resolved ones*. Broadly speaking, there are three procedures:

(1) *First procedure*. Medvedev and Greatbatch (2003, MG3) and before them, other authors (Geller et al., 1992), employed eddy resolving codes (in these cases, atmospheric codes) to obtain expressions for the unresolved mesoscale contributions. However, as noted in MG3, the procedure is not unique for it requires intermediate steps that are based more on mathematical arguments than on physics. The approach is nonetheless quite instructive in that MG3 employed eddy-resolving codes to provide not only second-order fluxes but also third-order moments, specifically, the flux of the temperature variance. In the ocean case, a similar approach was carried out by Bryan et al. (1999) (see below) but with the difference that a model for the mesoscale fluxes was first chosen and then tested.

(2) *Second procedure*. One can construct a *heuristic mesoscale model* to express the "mesoscale fluxes" in terms of the resolved scales. The validation of the mesoscale model can then be carried out by comparing its predictions against an eddy resolving ocean code or directly using it in a coarse resolution ocean model, OGCM and then comparing the results with a variety of data. The first type of test was used by several authors (Rix and Willenbrand, 1996; Bryan et al., 1999; Gille and Davis, 1999; Roberts and Marshall, 2000; Nakamura and Chao, 2000; Solovev et al., 2002). Use of an OGCM was carried out by Danabasoglu et al. (1994); Bonning et al. (1995), Gent et al. (1995) and by McDougall et al. (1996). The results exhibited a sharper thermocline, a cooler abyssal ocean, a more realistic latitudinal structure and magnitude of the polar heat transport, etc.

(3) *Third procedure*. One attempts to construct a dynamical mesoscale model by solving analytically the Navier–Stokes equations and the thickness equations. Clearly, this procedure requires approximations. Killworth (1997) considered the linearized case while here we present a model which includes the non-linearities which are treated with a turbulence model that was previously tested against a variety of turbulent data.

2. Equations for the mean variables

In isopycnal coordinates, and with the Boussinesq and adiabatic approximations, the dynamic equations for the two-dimensional velocity field $\mathbf{u}$ and the thickness h are ($a_t = \partial a/\partial t$):

$$\mathbf{u}_t + (\mathbf{u}\cdot\nabla)\mathbf{u} + f\mathbf{e}\times\mathbf{u} = -\rho_0^{-1}\nabla B \tag{1a}$$

$$h_t + \nabla\cdot(\mathbf{u}h) = 0 \tag{1b}$$

Here, h is the thickness and B is the linear Bernoulli function or Montgomery function:

$$h = \partial z/\partial\rho, \quad B \equiv p + g\rho z \tag{1c}$$

$f = 2\Omega\sin\phi$ is the Coriolis parameter, ϕ is the latitude and $\mathbf{e}$ is the unit vector along $-\nabla_3\rho$; ∇_3 is the 3D gradient operator and ∇ is the 2D gradient operator at constant density ρ. Due to the adiabatic approximation, the diapycnal component of the velocity field is neglected in (1a). This implies that the non-linear interactions act on isopycnal surfaces but not between them. The resulting isopycnal 2D flows interact among themselves only via the linear Bernoulli function B.

Using an overbar to denote a generic *Eulerian Mean*, *EM*, (temporal or spatial or a "mean" over a finite scale) and a prime to indicates the departure from the mean, e.g., $\mathbf{u} = \bar{\mathbf{u}} + \mathbf{u}'$, we obtain from Eqs. (1a) and (1b):

$$\bar{\mathbf{u}}_t + (f + \bar{\zeta})\mathbf{e}\times\bar{\mathbf{u}} = -\rho_0^{-1}\nabla_{\overline{B}_*} - \mathbf{e}\times\mathbf{F}_\zeta \tag{1d}$$

$$\overline{h}_t + \bar{\mathbf{u}}\cdot\nabla\bar{h} = -\nabla\cdot\mathbf{F}_h \tag{1e}$$

where $_{\overline{B}_*} = B + 1/2\rho_0\mathbf{u}^2$ and ζ is the relative vorticity. Thus, one must model *three mesoscale functions*: the thickness flux, the relative vorticity flux and the eddy kinetic energy K:

$$\mathbf{F}_h \equiv \overline{\mathbf{u}'h'}, \quad \mathbf{F}_\zeta \equiv \overline{\mathbf{u}'\zeta'}, \quad K = 1/2\overline{\mathbf{u}'^2} \tag{1f}$$

The main purpose of this work is to express the mesoscale functions (1f) in terms of the large scale fields. The forms of $\mathbf{F}_h$ and $\mathbf{F}_\zeta$ will be derived within the adiabatic approximation; however, the determination of K will require the inclusion of diabatic processes which allow a steady state to be reached (Section 13).

It may be instructive to make a connection with another representation *transformed eulerian mean*, the TEM, (Andrews and McIntyre, 1976, 1978; Plumb and Mahlman, 1987; Andrews et al., 1987, section 3) whereby one introduces the decomposition:

$$\mathbf{u} = \hat{\mathbf{u}} + \mathbf{u}'', \quad \hat{\mathbf{u}} = \overline{h\mathbf{u}}/\bar{h} = \bar{\mathbf{u}} + \bar{h}^{-1}\mathbf{F}_h = \bar{\mathbf{u}} + \mathbf{u}_* \tag{1g}$$

$$qh = f + \zeta, \quad q = \hat{q} + q'', \quad \bar{h}\hat{q} = \overline{qh} = f + \bar{\zeta} \tag{1h}$$

where q is potential vorticity and $\mathbf{u}_*$ is the bolus velocity (Rhines, 1982). Eqs. (1a) and (1b), and the ones for $\hat{q}$ and $\bar{h}$ now give

$$\frac{\partial}{\partial t}\bar{\mathbf{u}} + (f + \bar{\zeta})\mathbf{e}\times\hat{\mathbf{u}} = -\nabla_{\overline{B}_*} - \mathbf{e}\times\mathbf{F}_q \tag{1i}$$

$$\frac{\partial}{\partial t}\hat{q} + \hat{\mathbf{u}}\cdot\nabla\hat{q} = -\bar{h}^{-1}\nabla\cdot\mathbf{F}_q \tag{1j}$$

$$\overline{h}_t + \nabla\cdot(\bar{h}\hat{\mathbf{u}}) = 0 \tag{1k}$$

where $\mathbf{F}_q$ is the PV potential vorticity PV-flux defined as:

$$\mathbf{F}_q = \overline{hq''\mathbf{u}''} = \mathbf{F}_\zeta - \hat{q}\mathbf{F}_\mathrm{h} \tag{1l}$$

where the second relation follows directly from the above definitions. Since in Eq. (1k) there are formally no "eddy terms", if Eq. (1i) were prognostic in the variable $\hat{\mathbf{u}}$, there could be only two mesoscale terms to model, the PV-flux $\mathbf{F}_q$ that enters in both Eqs. (1i) and (1j) and the eddy kinetic energy K that enters the function $_{B_*}$. However, Eq. (1i) contains two velocities, $\bar{\mathbf{u}}$ and $\hat{\mathbf{u}}$, a fact common to many models (Tung, 1986; Andrews et al., 1987; Greatbatch, 1998, 2001). In this case, one must find a model to express the mesoscale variables corresponding to thickness flux, PV-flux and eddy kinetic energy:

$$\mathbf{F}_\mathrm{h}, \quad \mathbf{F}_q, \quad K \tag{1m}$$

in terms of large scale fields. In Section 4 we discuss a result of the model presented here that sheds some light on the relationship between $\mathbf{F}_\mathrm{h}$ and $\mathbf{F}_q$.

The outline of the paper is as follows. In Section 3, we give a brief summary of three major unsolved problems in mesoscale modeling. In Section 4 we present the key results we have obtained. In Section 5 we derive the equations for the turbulent fields describing the mesoscales. In Section 6 we discuss the conditions under which the non-linear interactions are important and in Section 7 we discuss the model we use to for them. In Section 8 we show that the set of mesoscale equations reduces to an eigenvalue problem for the mesoscale Bernoulli function, the solution of which is discussed in Section 9. In Sections 10 and 11, we give the expressions for the thickness and vorticity fluxes, Eq. (1m) while in Sections 12 and 13 we model the third variable of interest, the eddy kinetic energy K, Eq. (1f). In Section 14 we discuss several predictions of the model and comparison with the data. In Section 16 we draw some conclusions. The complete model is summarized in Appendix D.

3. Three unsolved problems in mesoscale models

3.1. Thickness vs. potential vorticity

Thus far, two heuristic models have been suggested to model the bolus velocity $\mathbf{u}_*$. The first by Gent and McWilliams (1990) is given by a down-gradient of the mean isopycnal thickness:

$$\mathbf{u}_* = -\kappa_\mathrm{M}\bar{h}^{-1}\nabla\bar{h} \tag{2a}$$

Here, κ_M is a mesoscale diffusivity that is not specified by the model. Other authors (Holland et al., 1984; Rhines and Young, 1982a,b; Lee et al., 1997; Greatbatch, 1998; McDougall and McIntosh, 1996, 2001; Killworth, 1997; Visbeck et al., 1997; Treguier et al., 1997; Treguier, 1999; Drijfhout and Hazeleger, 2001; Dukowicz and Greatbatch, 1999) have suggested instead the relation:

$$\mathbf{u}_* = \kappa_\mathrm{M}\hat{q}^{-1}\nabla\hat{q} \tag{2b}$$

the primary reason being the fact that q is a materially conserved quantity. It is still an open question whether (2a) or (2b) is the physically more correct representation of $\mathbf{u}_*$, if either.

3.2. Additional terms

A first hint as to the question just discussed came from the use of an eddy resolving code at 1/12° resolution by Bryan et al. (1999). The authors concluded that the isopycnal thickness flux $\mathbf{F}_h$ defined in (1f) has a non-zero divergence and a non-zero curl, while model (2a) with $\kappa_M = \text{constant}$ implies an $\mathbf{F}_h$ with zero curl. Moreover, the curl of $\mathbf{F}_h$ was shown to have a strength comparable with, if not larger than, that of the divergence. The conclusion of Bryan et al. (1999) was that the form of $\mathbf{u}_*$ is:

$$\mathbf{u}_* = \kappa_M \hat{q}^{-1} \nabla \hat{q} + \text{Additional terms} \tag{2c}$$

Even though Bryan et al. (1999) were not able to provide the form for the "additional terms", they were able to interpret them as an indication that "*the bolus velocity is more than just an agent of thickness mixing and flows are set up that are not closely linked to thickness source or sinks*". The presence of additional terms may explain the results of Roberts and Marshall (2000) who found no overwhelming evidence in support of (2b) in lieu of (2a) since both expressions are incomplete. Similarly, it may be at the root of Gille and Davis (1999) results showing that (2a) is still incomplete since the "skill index" is still only 40% (defined as the percentage of the mean squared mesoscale density flux divergence that is reproduced by the model). Finally, Solovev et al. (2002) concluded that (2a) "simulates the wrong sign of the divergences of the eddy heat flux in about half of the domain", in accord with previous results by Nakamura and Chao (2000). In addition, the presence of additional terms in (2c) makes it impossible to tune κ_M to simulate them. In conclusion, the nature of the additional terms is still unclear (Smith, 1999).

3.3. Mesoscale diffusivity κ_M

The z-dependence of κ_M or equivalently, its dependence on the resolved large-scale fields has been studied by several authors (Held and Larichev, 1996; Visbeck et al., 1997; Killworth, 1997; Treguier, 1999; Karsten and Marshall, 2002) but no unanimous outcome has yet emerged. An expression for the mesoscale diffusivity in terms of the resolved scales is thus needed.

4. Key results of the present model

Here, we present the main results we will derive in the following sections. The expressions for $\mathbf{F}_h$, Eqs. (17a) and (17b) contain two parts as in (2c), the first of which is the gradient of $\hat{q}$, while the "additional terms" have the form:

$$\text{Additional terms} = -\kappa_M \langle \hat{q}^{-1} \nabla \hat{q} \rangle - \kappa_M (1 + \sigma_t^{-1}) r_d^{-2} f^{-1} \mathbf{e} \times (\bar{\mathbf{u}} - \langle \bar{\mathbf{u}} \rangle) \tag{2d}$$

The average $\langle A(z) \rangle$ defined in Eq. (15d), is the integral over z of $A(z)$ with $K^{1/2}$ as the weight factor. In Eq. (2d) r_d is the Rossby deformation radius and σ_t is the turbulent Prandtl number. In accordance with the findings of Bryan et al. (1999), Eq. (2d) shows that the last two terms do not entail the gradients of either thickness/potential vorticity. The mesoscale diffusivity κ_M in Eq. (2d) is derived to have the form:

$$\kappa_{\mathrm{M}}(z) \sim r_{\mathrm{d}} K^{1/2}(z) \tag{2e}$$

The model for $K(z)$ is discussed in Sections 12 and 13; the predicted $\kappa_{\mathrm{M}}(z)$ from (2e) is similar to that derived from heuristic models (Karsten and Marshall, 2002), that is, it is the largest at the surface $\kappa_{\mathrm{M}}(0)$. In addition, the predicted value of $\kappa_{\mathrm{M}}(0)$ agrees with that of Karsten and Marshall (2002) who employed models of Holloway (1986) and Keffer and Holloway (1998) together with TOPEX Poseidon data for the sea surface height.

The bolus velocity (2c) and (2d) is shown to satisfy the baroclinic relation:

$$\int \mathbf{u}_*(z)\,\mathrm{d}z = 0 \tag{2f}$$

The mesoscale flux $\mathbf{F}_\zeta$, is given by Eq. (21):

$$\mathbf{F}_\zeta = K(1+\sigma_{\mathrm{t}})^{-1}\mathbf{ex}\langle \hat{q}^{-1}\nabla\hat{q}\rangle - K(\sigma_{\mathrm{t}} r_{\mathrm{d}}^2 f)^{-1}(\bar{\mathbf{u}} - \langle\bar{\mathbf{u}}\rangle + \mathbf{c}_{\mathrm{R}}) \tag{2g}$$

Here, $\mathbf{c}_{\mathrm{R}}$ is the velocity of the barotropic Rossby waves. Eq. (2g) contains both the gradient of the potential vorticity as well as terms that involve the mean flow velocity. The q-flux (1l) is then given by

$$\mathbf{F}_q = -\bar{h}\kappa_{\mathrm{M}}\nabla\hat{q} + \mathbf{F}_q^* \tag{2h}$$

with:

$$\mathbf{F}_q^* = \mathbf{F}_\zeta - \hat{q}\bar{h}(\text{Additional terms}) \tag{2i}$$

and where Eq. (2d) must be used to compute $\mathbf{F}_q^*$. The first term in $\mathbf{F}_q$ agrees with Rhines and Holland (1979) and Rhines and Young (1982a,b) conclusion that F_q "should have a down gradient component". In addition, Eq. (2i) provides an explicit form of the extra term.

Concerning the relation between $\mathbf{F}_{\mathrm{h}}$ and $\mathbf{F}_q$, in Section 11 we show that only the ageostrophic part of the mesoscale velocity field contributes to the relative vorticity flux $\mathbf{F}_\zeta$. Thus, if one assumes a geostrophic approximation, Eq. (1l) gives:

$$\mathbf{F}_q = -q\mathbf{F}_{\mathrm{h}} \tag{2j}$$

and thus only one mesoscale flux need to be modeled, for example the PV-flux together with the eddy kinetic energy K. However, as we show in Appendix B, the ageostrophic component of the velocity field is indispensable to close the so-called Lorenz energy cycle, specifically, the transformation of EKE (eddy kinetic energy) into EPE (eddy potential energy).

5. Dynamic equations for the turbulent fields

To derive the mesoscale dynamic equations from Eqs. (1a) and (1b), we separate the fields into a mean (represented by an overbar) and a fluctuating part (represented by a prime):

$$\mathbf{u} = \bar{\mathbf{u}} + \mathbf{u}', \quad h = \bar{h} + h', \quad B = \bar{B} + B' \tag{3}$$

Since $|\nabla\mathbf{u}'| \gg |\nabla\bar{\mathbf{u}}|$ we can neglect the isopycnal gradients $\partial\bar{u}_i/\partial x_j$. The equations for the fluctuating fields are derived to be:

$$\mathbf{u}'_{\mathrm{t}} + \bar{\mathbf{u}} \cdot \nabla \mathbf{u}' + f\mathbf{e} \times \mathbf{u}' = -\rho^{-1}\nabla B' + \mathbf{Q}(\mathbf{u}') \tag{4a}$$

$$h'_{\mathrm{t}} + \bar{\mathbf{u}} \cdot \nabla h' + \bar{h}\nabla \cdot \mathbf{u}' + \mathbf{u}' \cdot \nabla \bar{h} = Q(h') \tag{4b}$$

$$B'_{\rho} = gz', \quad h' \equiv z'_{\rho} \tag{4c,d}$$

where the Q's represent the non-linear terms, specifically:

$$\mathbf{Q}(\mathbf{u}') = \overline{\mathbf{u}' \cdot \nabla \mathbf{u}'} - \mathbf{u}' \cdot \nabla \mathbf{u}', \quad Q(h') = \nabla \cdot \overline{\mathbf{u}' h'} - \nabla \cdot \mathbf{u}' h' \tag{4e}$$

The linear version of Eqs. (4) corresponding to $Q = 0$ was studied by Killworth (1997). Next, we Fourier transform the fields on an isopycnal surface around the origin defined by the 2D radius vector $\mathbf{r}_0$ while $\mathbf{r}$ denotes a variable radius from the same origin. Since the large scale fields $\bar{\mathbf{u}}$, $\bar{h}$, ∇h almost do not change on the scales characterizing the mesoscale eddies, we consider them constant. As for the Coriolis parameter f, we take into account its variability via the relation $f = f_0 + \boldsymbol{\beta} \cdot \mathbf{r}$ where $\boldsymbol{\beta} = \nabla f$ and f_0 is the value of f at the origin and $\boldsymbol{\beta}$ is directed along a meridian. Let us take the space and time Fourier transforms of Eqs. (4a) and (4b). When doing so, in the third term in Eq. (4a) the function f is substituted by the operator:

$$\hat{f} = f_0 + \mathbf{i}\boldsymbol{\beta} \cdot \frac{\partial}{\partial \mathbf{k}} \tag{4f}$$

We further split the fluctuating mesoscale velocity field into solenoidal (divergence free) and potential (curl free) components:

$$\mathbf{u}'(\mathbf{k}) = \mathbf{u}_{\mathrm{s}}(\mathbf{k}) + \mathbf{u}_{\mathrm{p}}(\mathbf{k}), \tag{4g}$$

where

$$\mathbf{n} = \mathbf{k}/k, \quad \mathbf{n} \cdot \mathbf{u}_{\mathrm{s}}(\mathbf{k}) = 0, \quad \mathbf{n} \times \mathbf{u}_{\mathrm{p}}(\mathbf{k}) = 0 \tag{4h}$$

and thus:

$$\mathbf{u}_{\mathrm{s}}(\mathbf{k}) = \mathbf{n} \times \mathbf{e}u_{\mathrm{s}}(\mathbf{k}), \quad \mathbf{u}_{\mathrm{p}}(\mathbf{k}) = \mathbf{n}u_{\mathrm{p}}(\mathbf{k}) \tag{4i}$$

Using Eqs. (4g) and (4h), the equations for the scalars velocities $u_{\mathrm{s}}(\mathbf{k})$ and $u_{\mathrm{p}}(\mathbf{k})$ and Eq. (4b) become:

$$-\mathrm{i}\omega u_{\mathrm{s}} = -\mathrm{i}\mathbf{k} \cdot (\bar{\mathbf{u}} + \mathbf{c}_{\mathrm{R}})u_{\mathrm{s}} + \hat{f}u_{\mathrm{p}} + Q_{\mathrm{s}} \tag{5a}$$

$$-\mathrm{i}\omega u_{\mathrm{p}} = -\mathrm{i}\mathbf{k} \cdot (\bar{\mathbf{u}} + \mathbf{c}_{\mathrm{R}})u_{\mathrm{p}} - \hat{f}u_{\mathrm{s}} - \mathrm{i}k\rho^{-1}B' + Q_{\mathrm{p}} \tag{5b}$$

$$-\mathrm{i}\omega h' = -\mathrm{i}(\mathbf{k} \cdot \bar{\mathbf{u}})h' - \mathrm{i}\bar{h}ku_{\mathrm{p}} - \mathbf{n} \cdot \nabla \bar{h}u_{\mathrm{p}} + (\mathbf{e} \times \mathbf{n})\nabla \bar{h}u_{\mathrm{s}} + Q_{\mathrm{h}} \tag{5c}$$

where $\mathbf{c}_{\mathrm{R}}$ is the velocity of the barotropic Rossby waves:

$$\mathbf{c}_{\mathrm{R}} = k^{-2}\mathbf{e} \times \nabla f = k^{-2}\mathbf{ex}\boldsymbol{\beta} \tag{5d}$$

The $\mathbf{c}_{\mathrm{R}}$ term in Eqs. (5a) and (5b) comes from acting with the second term in (4f) upon the unit vector $\mathbf{n}$ in (4g) and (4h). Notice that after the Fourier transformation, the gradient of the Bernoulli function in Eq. (4a) has only one component along $\mathbf{k}$. As a result, the Bernoulli term is absent in Eq. (5a) which is the projection of the Fourier transformed equation (4a) onto the direction $\mathbf{kxe}$. Below, we shall show that the solenoidal and potential components $u_{\mathrm{s,p}}$ will coincide

with the geostrophic (subscript g) and ageotrophic (subscript a) components of the mesoscale velocity field:

$$u_s = u_g, \quad u_p = u_a \tag{5e}$$

In Eqs. (5a) and (5b) we can neglect the second term in$\hat{f}$ defined in (4f) since $\beta L_e \sim 10^{-1} s^{-1} \ll f$, where L_e is a typical eddy size. However, if we had neglected such a term everywhere we would have missed the β-term that gives rise to the Rossby velocity $\mathbf{c}_R$, a term that becomes important in Eq. (5a) when $u_s \gg u_p$ which indeed characterizes the mesoscale field, as we discuss below, Eq. (7a). To simplify the notation, we shall use f instead of f_0 henceforth.

6. When are the non-linear terms important?

Here we discuss under what conditions the non-linear interactions can be neglected compared to other terms in the Eqs. (5a)–(5c). For simplicity, we consider the case:

$$\bar{\mathbf{u}} = 0, \quad \nabla \bar{h} = 0 \tag{6a,b}$$

6.1. High frequency inertial gravity waves $\omega > f$

In this limit, Eqs. (5a)–(5d) yield gravity-inertial waves. Neglecting $\mathbf{c}_R$, the dispersion relation is:

$$\omega^2 = f^2(1 + k^2 r_n^2) \tag{6c}$$

where r_n is the set of eigenvalues (Rossby deformation radii) obtained by solving the eigenvalue problem:

$$\partial_{\rho\rho} B_n + \lambda_n^2 B_n = 0, \quad \lambda_n = N\bar{h}/r_n f \tag{6d}$$

where N is the Brunt–Vaisala frequency, $N^2 = -(g\bar{h}\rho_0)^{-1}$. Since for mesoscale eddies we have that $k_0^{-1} \sim r_d = r_1$, from (5a) we derive that $\omega \sim f$ and $u_s \sim u_p$. Since $Q_s \sim Q_p \sim u_s^2 \ell^{-1}$, the ratio of the last two terms in (5a) is given by

$$Q_s (f u_s)^{-1} \sim u_s (f\ell)^{-1} \sim Ro_t \tag{6e}$$

where Ro_t is the turbulent Rossby number. For ocean mesoscale eddies with characteristic values $u_s \sim 10^{-1}$ ms^{-1}, $\ell \sim 10^2$ km and $f \sim 10^{-4}$ s^{-1}, we obtain $Ro_t \ll 1$ and thus Q_s is smaller than the Coriolis terms in (5a) and (5b); $Q_h \sim uh' r_d^{-1}$ is much smaller than $\omega h' \sim f h'$ since $u_s r_d^{-1} \sim 3 \times 10^{-6} s^{-1} \ll f$. We conclude that in this case, the Q's are unimportant.

6.2. Low frequency Rossby waves $\omega \ll f$

The low frequency solution of Eq. (5a) yields:

$$u_s \gg u_p \tag{7a}$$

In this case, under conditions (6a,b), Eqs. (5) yield Rossby waves with the dispersion relation:

$$\omega = -\beta(\mathbf{e}_x \cdot \mathbf{k}) r_n^2 (1 + k^2 r_n^2)^{-1} \sim \beta\ell \tag{7b}$$

where r_n are the solutions of Eq. (6d). Proceeding as above, we derive the relations:

$$Q_s/(kc_R u_s) \sim u_s/c_R, \quad Q_s/(\omega u_s) \sim u_s/(\omega \ell) \sim u_s/(\beta \ell^2) \sim u_s/c_R \tag{7c}$$

Since from (5d) we have $c_R \sim 10^{-2}$ ms^{-1} and since $u_s \sim 10^{-1}$ ms^{-1}, the ratios (7c) are larger than unity. In this case the *non-linear terms Q_s are not smaller than the other terms and must be retained.* This means that the ensuing turbulent flow can be viewed as a system of "broken", low frequency, Rossby waves.

7. Modeling the non-linear interactions

To treat the non-linear terms, we use a turbulence model that was previously tested in a large variety of flows that included shear flows, buoyancy flows, 2D turbulence, turbulence under strong rotation, freely decaying turbulence, etc., for a total of about 80 turbulence statistics (Canuto and Dubovikov, 1996a,b,c, CD96).

The CD model predicts the generation of coherent states (CS) whose lifetime is longer than the turbulent time ℓ/w, where ℓ and w are typical eddy sizes and velocity. For example, in the case of Benard convection, CS are large-scale coherent loop-like flows circulating between opposite plates (Wu and Libchaber, 1992; Ciliberto et al., 1996). In the ocean, CS are the mesoscale eddies. Since there is no diapycnal mass transfer between layers of different densities, the Q-terms operate only inside the layers that interact among themselves through the term ikB' in Eq. (5b). In each isopycnal layer we can therefore employ a 2D turbulence model.

In standard 2D turbulence, both energy and enstrophy (square of relative vorticity) are conserved which entails an upscale energy cascade and a downscale enstrophy cascade. However, in the present context of geostrophic turbulence, what is conserved is potential rather than relative vorticity. As discussed in detail in Section 15, relative vorticity is conserved (with an enstrophy cascade) **only** for scales $\ell_1 \ll r_d$ The absence of an enstrophy cascade in the range r_d–ℓ_1 assures that only an inverse energy cascade is possible. Mathematically, this is represented by a negative viscosity.

Taking into account a negative viscosity but a positive diffusivity, the CD model yields for the Q's in the vicinity of the maxima k_0 of the spectra the following results:

$$Q_s(\mathbf{k}) = \tilde{\nu}_t u_s(\mathbf{k}), \quad Q_p(\mathbf{k}) = \tilde{\nu}_t u_p(\mathbf{k}), \quad Q_h(\mathbf{k}) = -\tilde{\chi}_t h'(\mathbf{k}) \tag{8a}$$

$$\tilde{\nu}_t \equiv k_0^2 \nu_t(k_0), \quad \tilde{\chi}_t \equiv k_0^2 \chi_t(k_0) \tag{8b}$$

$$\nu_t(k) = \nu\left[1 + \frac{1}{2}\nu^{-2}\int_k^\infty p^{-2}E(p)\,dp\right]^{1/2}, \quad \chi_t(k) = \sigma_t^{-1}\nu_t(k) \tag{9a}$$

where $E(p)$ is the energy spectrum and $\sigma_t = 0.72$ is the turbulent Prandtl number (the value was derived in CD96). The expression for the turbulent viscosity $\nu_t(k)$ can also be written as:

$$\nu_t(k) = \nu[1 + Re^2(k)]^{1/2} \tag{9b}$$

where $Re(k) \sim U(\ell)\ell\nu^{-1} \sim [E(k)\Delta k]^{1/2}(k\nu)^{-1}$ is a wave-number dependent Reynolds number. It may be noticed that for large Re, $\nu_t/\nu = Re$, as expected. From Eqs. (9a) we have that for $\nu_t > \nu$:

$$\tilde{\nu} = \sigma_t \tilde{\chi} = C k_0 K^{1/2} \tag{9c}$$

where $C \sim 1$ and K is the eddy kinetic energy. Data from Stammer (1997, 1998) show that $|\bar{\mathbf{u}}| \sim 10^{-2}$ cm s^{-1}, $u \sim 10^{-1}$ ms^{-1} and thus K is larger than the mean flow kinetic energy, MKE. This means that $(\tilde{\nu}, \tilde{\chi}) > |\mathbf{k} \cdot \bar{\mathbf{u}}|$. Since we show below that $\omega \sim \mathbf{k} \cdot \mathbf{u}$ and since $c_R \sim 10^{-2}$ ms^{-1}, the time scales of the problem satisfy the following relations:

$$|\mathbf{k} \cdot \mathbf{c}_R| \leqslant |\mathbf{k} \cdot \bar{\mathbf{u}}| \sim |\omega| < \tilde{\nu}, \tilde{\chi} < f \tag{9d}$$

where $k_0^{-1} \sim r_d \sim 30$ km. The last inequality follows from the fact that even for the most energetic eddies with $K \sim 0.2$ m^2 s^{-1}, we have $\tilde{\nu} \leqslant 10^{-5}$ s^{-1} which is an order of magnitude smaller than $f \cong 10^{-4}$ s^{-1}. Using (9c), the second and fourth terms of (9d) also imply that:

$$|\bar{\mathbf{u}} < |\mathbf{u}'| \tag{9e}$$

8. Dynamic equations for mesoscale eddies

To derive the equations for the mesoscale eddies, we substitute the CD expression (8) into (5a)–(5c). Eq. (5a) becomes

$$-f u_p = \{\tilde{\nu} - i[\mathbf{k} \cdot (\bar{\mathbf{u}} + c_R) - \omega]\} u_s \tag{10a}$$

Due to (7a) and (9d), the last three terms in Eq. (5b) dominate. However, due to (7a) and the last inequality in (9d) and the expression (8a) for Q_p; the latter is three orders of magnitude smaller than the other two terms. Eq. (5b) then becomes:

$$f u_s = -ik\rho^{-1} B', \quad z' = g^{-1} B'_\rho \tag{10b}$$

which is the geostrophic relation in isopycnal coordinates. In Eqs. (5c) we can neglect the term $-\mathbf{n} \cdot \nabla \bar{h} u_p$ which, because of (7a), is small compared with $(\mathbf{e} \times \mathbf{n}) \cdot \nabla \bar{u} h' u_s$. That term is also smaller than the term $i\bar{h} k u_p$ by more than an order of magnitude since the ratio of these terms is of order $(k_0 L)^{-1} \sim r_d L^{-1} \sim 3 \times 10^{-2}$, where $L \sim 10^3$ km is the size of the large-scale fields. Thus, Eq. (5c) becomes:

$$-i\omega h' = -i\mathbf{k} \cdot \bar{\mathbf{u}} h' + (\mathbf{e} \times \mathbf{n}) \nabla \bar{h} u_s - i\bar{h} k u_p - \tilde{\chi} h' \tag{10c}$$

Eliminating u_s, u_p, h' and z' between (10a)–(10c), we obtain a single equation for the function $B' = B'(\mathbf{k}, \rho, \omega)$ computed at $k = k_0$.

$$\left(\frac{\partial^2}{\partial \rho^2} + \Lambda \right) B' = 0 \tag{11a}$$

where we have defined the following variables:

$$\Lambda = \lambda^2 \bar{h}^2 (1 - i\Omega_1 \tau)^{-1} (1 + i\Omega_2 \tau) \tag{11b}$$

$$\lambda^2 \equiv \sigma_t k_0^2 N^2 f^{-2}, \quad N^2 = -(g\bar{h}\rho_0)^{-1} \tag{11c}$$

$$\tau \equiv \tilde{\chi}^{-1} + \tilde{\nu}^{-1} = \tilde{\chi}^{-1} (1 + \sigma_t^{-1}) \tag{11d}$$

$$\Omega_1 = (1 + \sigma_t^{-1})^{-1} (\omega - \mathbf{k} \cdot \bar{\mathbf{u}}), \quad \Omega_2 = (1 + \sigma_t)^{-1} (\omega - \mathbf{k} \cdot \widetilde{\mathbf{V}}) \tag{11e}$$

$$\widetilde{\mathbf{V}} = \bar{\mathbf{u}} + \mathbf{c}_{\mathrm{R}} - f(k_0^2\bar{h})^{-1}\mathbf{e}\times\nabla\bar{h} \tag{11f}$$

*Eq. (*11a*) constitutes the vertical eigenvalue problem for B' with eigenvalues k_0 and ω*. Using Eqs. (9c) and (9d), it turns out that $\tau\Omega_{1,2} \sim \bar{\mathbf{u}}K^{-1/2} < 1$. Thus, up to second-order in $\tau\Omega_{1,2}$, Eqs. (11b), (11d) and (11f) simplify to:

$$\Lambda = \lambda^2\bar{h}^2(1+\mathrm{i}\Omega\tau), \quad \tau^{-1} = \frac{1}{5}k_0K^{1/2} \tag{12a}$$

$$\Omega = \omega - \mathbf{k}\cdot\mathbf{V}, \quad \mathbf{V} \equiv \bar{\mathbf{u}} + (1+\sigma_{\mathrm{t}})^{-1}\mathbf{c}_{\mathrm{R}} - f[(1+\sigma_{\mathrm{t}})\bar{h}k_0^2]^{-1}\mathbf{e}\times\nabla\bar{h} \tag{12b}$$

With the boundary conditions $B'_\rho(\rho_{\mathrm{b}}) = 0$ and $B'_\rho(\rho_{\mathrm{t}}) = 0$ (Killworth, 1997), where the subscripts (b,t) stand for bottom and top, the eigenvalue equation (11a) is complete.

9. Solution of the eigenvalue problem

We solve (11a) perturbatively in powers of $\Omega\tau$, namely we write (for simplicity we will omit the prime in B') $B = b_0 + b_1 + \cdots$. In the zeroth- and first-order, one has the relations:

$$\widehat{L}_0 b_0 = 0, \quad \widehat{L}_0 b_1 = -\mathrm{i}\Omega\tau b_0, \quad \widehat{L}_0 \equiv 1 + (\lambda\bar{h})^{-2}\frac{\partial^2}{\partial\rho^2} \tag{13a}$$

From Eqs. (11a) and (12a), it follows that the function b_0 must coincide with one of the eigenfunctions B_n solutions of the eigenvalue problem Eq. (6d). The eddy size $L_{\mathrm{e}} \equiv \pi/k_0$ is determined by the eigenvalue r_n given by

$$k_0^{-1} = \sigma_{\mathrm{t}}^{1/2} r_n \tag{13b}$$

In Eq. (13b), the non-linear interactions only enter through the largely constant ratio of the turbulent viscosity to the turbulent conductivity $\nu_{\mathrm{t}}/\chi_{\mathrm{t}} = \sigma_{\mathrm{t}}$. Only $n = 1$ is consistent with the measured data and $r_1 = r_{\mathrm{d}}$ is the first Rossby deformation radius. Since $\sigma_{\mathrm{t}} \sim \mathrm{O}(1)$, we have $L_{\mathrm{e}} \sim 3r_{\mathrm{d}}$, in agreement with the data (Stammer, 1997, 1998). With these premises, next we use the expansion:

$$b_0 = a_1 B_1, \quad b_1 = \sum_0^\infty{}^* a_n B_n \tag{14a}$$

where $\sum^*$ means that the B_1 term is absent. It is easy to prove that the eigenfunctions B_n, B_m are orthogonal with the weight factor $\bar{h}$:

$$\int B_n^* B_m \bar{h}\,\mathrm{d}\rho = c_n\delta_{nm} \tag{14b}$$

where c_n are normalization factors. In addition, since the operator in (13a) is real, we can choose the B_n to be real as well. Substituting (14a) into the second of (13a), multiplying by $\bar{h}B_1$, integrating over ρ and using (14b), we obtain:

$$\int_{\rho_{\mathrm{t}}}^{\rho_{\mathrm{b}}} |B_1|^2\Omega\tau\bar{h}\,\mathrm{d}\rho = 0 \tag{14c}$$

Substitution of Ω from (12b) yields the eigenvalue ω:

$$\omega = \mathbf{k} \cdot \mathbf{u}_{\mathrm{d}} \tag{15a}$$

where

$$\mathbf{u}_{\mathrm{d}} = \langle \bar{\mathbf{u}} \rangle - (1 + \sigma_{\mathrm{t}}^{-1})^{-1} f r_{\mathrm{d}}^2 \mathbf{e} \times \langle \bar{h}^{-1} \nabla \bar{h} \rangle + (1 + \sigma_{\mathrm{t}})^{-1} \mathbf{c}_{\mathrm{R}} \tag{15b}$$

or, using Eqs. (5d) and (13b):

$$\mathbf{u}_{\mathrm{d}} = \langle \bar{\mathbf{u}} \rangle + \sigma_{\mathrm{t}} (1 + \sigma_{\mathrm{t}})^{-1} f r_{\mathrm{d}}^2 \mathbf{e} x \langle \hat{q}^{-1} \nabla \hat{q} \rangle \tag{15c}$$

which shows that $\mathbf{u}_{\mathrm{d}}$ is barotropic (z-independent) but depends on location. The average $\langle X \rangle$ is defined as:

$$\langle X \rangle \equiv \int_{\rho_{\mathrm{t}}}^{\rho_{\mathrm{b}}} X \Gamma^{-1/2} |B_1|^2 \bar{h} \, \mathrm{d}\rho \left(\int_{\rho_{\mathrm{t}}}^{\rho_{\mathrm{b}}} \Gamma^{-1/2} |B_1|^2 \bar{h} \, \mathrm{d}\rho \right)^{-1} \tag{15d}$$

where

$$\Gamma(\rho) \equiv K(\rho)/K_{\mathrm{t}} \tag{15e}$$

is the mesoscale kinetic energy normalized to its surface value K_{t} (the subscript t stands for top). $\Gamma(\rho)$ will be discussed later while $B_1(z)$ is solution of Eq. (6d).

10. Thickness flux Bolus velocity

Of the three mesoscale variables in Eq. (1m), we begin to compute the first, the thickness flux:

$$\mathbf{F}_{\mathrm{h}} = \overline{\mathbf{u}' h'} = \int \mathbf{F}_{\mathrm{h}}(k) \, \mathrm{d}k \tag{16a}$$

Since Eqs. (10) show that all fields are related to one another, they can all be expressed in terms of only one of them. Thus, all second-order correlations can be expressed in terms of the energy spectrum $E(k)$. As shown in Appendix A, this yields the following results:

$$\mathbf{F}_{\mathrm{h}}(k) = -(1 + \sigma_{\mathrm{t}}^{-1})^{-1} \tau E(k) \bar{h} \boldsymbol{\Psi} \tag{16b}$$

$$\boldsymbol{\Psi} = \bar{h}^{-1} \nabla \bar{h} + (1 + \sigma_{\mathrm{t}}^{-1}) r_{\mathrm{d}}^{-2} f^{-1} \mathbf{e} \times [\bar{\mathbf{u}} - \mathbf{u}_{\mathrm{d}} + (1 + \sigma_{\mathrm{t}})^{-1} \mathbf{c}_{\mathrm{R}}] \tag{16c}$$

Though Eqs. (16b) and (16c) are valid near k_0, we extend them to the whole energy-containing region under the reasonable assumption that the widths of the spectra do not differ greatly. The integration over k is then equivalent to substituting $E(k)$ with K. We obtain:

$$\mathbf{F}_{\mathrm{h}} = \bar{h} \mathbf{u}_*, \quad \mathbf{u}_* = -\kappa_{\mathrm{M}} \boldsymbol{\Psi}, \quad \kappa_{\mathrm{M}} = (1 + \sigma_{\mathrm{t}}^{-1}) \tau K \tag{17a}$$

The vector $\boldsymbol{\Psi}$ can be presented in two forms. Using the mean potential vorticity $\hat{q}$ defined in (1h), one obtains:

$$\boldsymbol{\Psi} = -\hat{q}^{-1} \nabla \hat{q} + \langle \hat{q}^{-1} \nabla \hat{q} \rangle + (1 + \sigma_{\mathrm{t}}^{-1}) r_{\mathrm{d}}^{-2} f^{-1} \mathbf{e} \times (\bar{\mathbf{u}} - \langle \bar{\mathbf{u}} \rangle) \tag{17b}$$

Alternatively, we have:

$$\mathbf{\Psi} = \bar{h}^{-1}\nabla\bar{h} - \langle\bar{h}^{-1}\nabla\bar{h}\rangle + (1+\sigma_t^{-1})r_d^{-2}f^{-1}\mathbf{e}\times(\bar{\mathbf{u}} - \langle\bar{\mathbf{u}}\rangle) \tag{17c}$$

We notice that the β-terms contained in the mean vorticity q are depth independent and thus cancel out in going from (17b) to (17c). The mesoscale diffusivity is obtained by substituting (12a) and (13b) into (17a) and by using the value $\sigma_t = 0.72$. The result is:

$$\kappa_M = 1.8 s^{1/2} r_d K^{1/2}(z) \tag{18}$$

where we have added the filling factor "s" to represent the fraction of the flow's area occupied by the mesoscale eddies. (17–18) *are the expressions for the thickness flux, bolus velocity and mesoscale diffusivity*. Using Eqs. (17a–c) and (15d,e) it is easy to verify that $\mathbf{u}_*$ satisfies the relation:

$$\int \mathbf{u}_*(z)\,dz = 0 \tag{19}$$

showing that $\mathbf{u}^*$ is a baroclinic variable.

11. Relative vorticity flux, potential vorticity flux

Next, consider the second mesocale variable in Eq. (1m), the relative vorticity flux:

$$\mathbf{F}_\zeta \equiv \overline{\mathbf{u}'\zeta'} \tag{20a}$$

First, we employ the vorticity flux in k-space:

$$\delta(\mathbf{k}-\mathbf{k}')\widetilde{\mathbf{F}}_\zeta(\mathbf{k}) = Re\overline{\overline{\mathbf{u}'}^*(\mathbf{k}')\zeta'(\mathbf{k})} \tag{20b}$$

Using the definition of ζ and the decomposition (4g) and (4h), we derive that:

$$\zeta'(\mathbf{k}) = -\mathrm{i}k u_s(\mathbf{k}) \tag{20c}$$

Because of the presence of i in (20c) only $u_p(k)$, the potential (ageostrophic) part of $\mathbf{u}'(\mathbf{k})$, contributes to (20b). Using (10b) and (15a), we finally obtain that near $k \sim k_0$:

$$\delta(\mathbf{k}-\mathbf{k}')\widetilde{\mathbf{F}}_\zeta(\mathbf{k}) = -f^{-1}k_0^{-1}\mathbf{n}\mathbf{k}\cdot(\bar{\mathbf{u}} - \mathbf{u}_d + \mathbf{c}_R)\overline{u(\mathbf{k})u^*(\mathbf{k}')} \tag{20d}$$

The vorticity spectrum $\mathbf{F}_\zeta(k)$ is related to $\widetilde{\mathbf{F}}_\zeta(\mathbf{k})$ as follows:

$$\mathbf{F}_\zeta(k) = k\int \widetilde{\mathbf{F}}_\zeta(\mathbf{k})\,d\mathbf{n} \tag{20e}$$

Using the same procedure that led to $\mathbf{F}_h$, we obtain:

$$\mathbf{F}_\zeta = K(1+\sigma_t)^{-1}\mathbf{e}x\langle\hat{q}^{-1}\nabla\hat{q}\rangle - K(\sigma_t r_d^2 f)^{-1}(\bar{\mathbf{u}} - \langle\bar{\mathbf{u}}\rangle + \mathbf{c}_R) \tag{21}$$

For completeness, we also construct the PV-flux, Eq. (1l). With Eqs. (21) and (17a,b), we obtain:

$$\mathbf{F}_q = -\bar{h}\kappa_M\nabla\hat{q} + \mathbf{F}_q^* \tag{22a}$$

where

$$\mathbf{F}_q^* = \mathbf{F}_\zeta - \hat{q}\bar{h}\kappa_M[\langle\hat{q}^{-1}\nabla\hat{q}\rangle + (1+\sigma_t^{-1})r_d^{-2}f^{-1}\mathbf{e}\times(\bar{\mathbf{u}} - \langle\bar{\mathbf{u}}\rangle)] \tag{22b}$$

The PV-flux is contributed by two terms. The first term is the gradient of the mean PV and confirms the results of Rhines and Holland (1979), and Rhines and Young (1982a,b) that the q-flux "should have a down-gradient term". The remaining term contains contributions from the relative vorticity flux, the z-averaged PV-gradient and the mean flow.

12. Mesoscale kinetic energy: part A

Last, we derive an expression for the eddy kinetic energy, Eq. (1m). Since the derivation is rather complex, we divided the task into two parts. In part A, we derive an expression of the ratio (15e) of the eddy kinetic energy to its surface values and in part B we derive an expression for the surface value K_t.

Using the normalization $B_n(\rho_s) = 1$ in (14b), from Eqs. (7a) and (14a), it follows that $a_1 = 1$ and so:

$$\Gamma(\rho) = |B_1 + \Sigma' a_n B_n|^2 |1 + \Sigma a_n|^{-2} \tag{23a}$$

where the B_n's are functions of ρ. The zeroth-order approximation, corresponding to taking all $a_n = 0$, is not sufficient since $B_1(\rho)$ vanishes at some ρ^*. From Eqs. (14a) and (14b) it follows that:

$$a_n = c_n^{-1} \int \bar{h} b_1(\rho) B_n^*(\rho)\, \mathrm{d}\rho \tag{23b}$$

At the same time, from Eqs. (13a) and (6c), one has:

$$A_n a_n c_n = \mathrm{i} \int \Omega \tau B_1 B_n^* \bar{h}\, \mathrm{d}\rho \tag{23c}$$

where

$$A_n = r_d^2 / r_n^2 - 1 \tag{23d}$$

Using the WKB method, it can be shown that $r_n \sim r_d/n$ and thus $A_n \sim n^2 - 1$. From Eqs. (23b)–(23d) it follows that the a_n decrease quite rapidly with increasing n. In reality, the decrease is even faster than the above analysis indicates since the eigenfunctions B_n oscillate quite rapidly thus reducing their contribution to the integral in (23b). Thus, the main contribution to the sums in (23a) comes from $n = 0$. In addition, since $B_0 = 1$, only these terms are important since all $B_n(\rho)$ with $n \geqslant 2$ decrease when $\rho \geqslant \rho^*$, where the correction to the zeroth-order is essential. Finally, since the operator in (6c) is real and hermitian, we can choose the B_n to be real as well. From (23b) and (23c) it follows that the a_n must be purely imaginary. Combining Eqs. (23a,b), (11d), (12b), (15a,b) and (17c), we obtain:

$$\frac{K}{K_t} \equiv \Gamma(\rho) = \left(|B_1|^2 + |a_0|^2\right)\left(1 + |a_0|^2\right)^{-1} \tag{24a}$$

where

$$|a_0|^2 = 2 f^2 r_d^4 \mathbf{j}^2 \quad \mathbf{j} = H^{-1} \int \bar{h} K^{-1/2} B_1(\rho) \boldsymbol{\Psi}\, d\rho \tag{24b,c}$$

where H is ocean's depth, $\mathbf{\Psi}$ is given by Eqs. 17b,17c and $B_1(\rho)$ is solution of Eq. (6d). The kinetic energy K appearing in (24c) can be approximated as follows. Since the term a_0 in (24a) represents a correction to the zero order approximation:

$$\Gamma_0(\rho) = |B_1|^2 \tag{24d}$$

we may substitute (24d) into (24c). Using (24d), we can represent $B_1(\rho)$ as:

$$B_1(\rho) = \theta(\rho_* - \rho)\Gamma_0(\rho)^{1/2} \tag{24e}$$

where $\theta(x) = \pm 1$ for $x > 0$ and $x < 0$. Substitution of (24e) and (15d) into (24b,c) gives:

$$|a_0|^2 = 2f^2 r_{\mathrm{d}}^4 K_{\mathrm{t}}^{-1} \mathbf{J}^2 \tag{25}$$

$$\mathbf{J} = H^{-1} \int \theta(\rho^* - \rho)\mathbf{\Psi}\bar{h}\,\mathrm{d}\rho \tag{26}$$

The problem of expressing the ratio K/K_{t} is thus complete: it is given by relations (24a), (25) and (26) while B_1 is given by solving (6d).

13. Mesoscale kinetic energy: part B

The well-known Lorenz cycle (Holton, 1992, fig. 10.13) represents the observed energy cycle among eddies and their sources, the baroclinic instabilities (Appendix B and Fig. 1). A key feature to be noticed is that mean kinetic energy (MKE) transforms into mean potential energy (MPE), not vice versa. As a result, MPE is two orders of magnitude larger than MKE. This is because at large scales, the Rossby number is very small and the (almost geostrophic) large-scale mean velocity is orthogonal to the gradient of the mean potential energy and the latter performs no work. Let us denote by P_{b} the production of eddy potential energy (EPE) by baroclinic instabilities at r_{d} (process 1, Fig. 1). Lorenz cycle simply states that EPE is then converted to EKE (eddy kinetic energy). At first, this seems surprising since the previous argument about the absence of work by the mean potential energy holds true for the eddy potential energy as well. The Lorenz model does not provide the details of how the EPE $\rightarrow$ EKE conversion occurs. In the present model, EPE first cascades from large to small scales (process 2). This leads to the EPE $\rightarrow$ EKE conversion (process 3a) only at scales sufficiently small (called k_1 in Fig. 1) where the Rossby number has becomes of order unity. The size of the scales at which this occurs $\ell_1 \sim k_1^{-1}$ follows from the condition that the corresponding turbulent time scale τ be of the order of the Coriolis time scale $\tau f \sim 1$; a typical value is $\ell_1 \sim 1$ km. Process 3a is however not the only process occurring at these scales since there is also an irreversible dissipation (process 3b). The EKE thus generated has an inverse cascade (process 4) toward larger scales until scales of order $k_{\mathrm{d}} \sim r_{\mathrm{d}}^{-1}$ where, *via the ageostrophic velocity field* u_{p}, energy gets exchanged between the velocity and the h field (processes 5,6). This energy is an addition to the one originating from the large scale baroclinic instabilities.

To obtain an expression for P_{b}, let us denote by $\varepsilon_{p,k}$ the fluxes of potential and kinetic energies while ε_{d} is the dissipation (which is zero under adiabatic conditions). Energy conservation applied to the left and right hand sides of Fig. 1 yields:

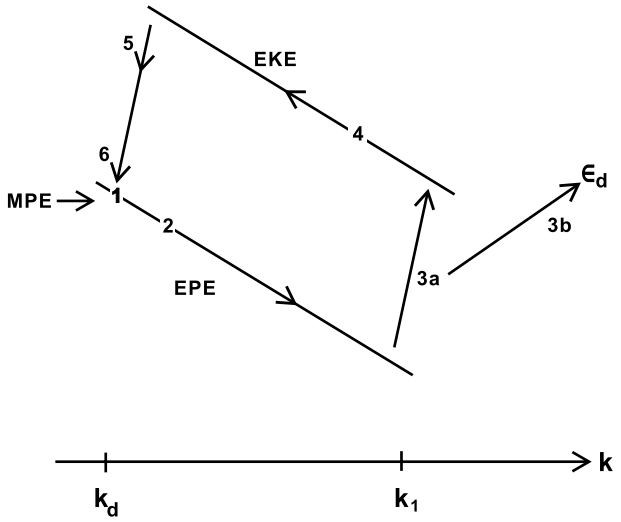

Fig. 1. The energy exchange cycle discussed in Appendix B.

$$P_b + \int \varepsilon_k \, dz = \int \varepsilon_p \, dz, \quad \int (\varepsilon_p - \varepsilon_d - \varepsilon_k) \, dz = 0 \tag{27a}$$

If we call $\tilde{\eta} = \varepsilon_d/\varepsilon_p$ the fraction of eddy potential energy that goes into the dissipative process 3b of Fig. 1, Eqs. (27a) can be combined to give:

$$P_b = \eta^{-1} \int \varepsilon_k \, dz, \quad \eta \equiv \tilde{\eta}^{-1} - 1 \tag{27b}$$

Since Kolmogorov's law relates ε_k to K which we consider known, we need to compute P_b. If U is the potential energy per unit horizontal area (to simplify the notation, all integrals on ρ will be understood to have lower and upper limits ρ_b and ρ_t), we have:

$$EPE = \int U \, d^2\mathbf{r}, \quad U = \frac{1}{2} g \int \overline{z'^2} \, d\rho \tag{28a}$$

and since $z' = g^{-1} B'_\rho$, use of the boundary conditions $B'_b(\rho) = B'_t(\rho) = 0$ gives (we omit the primes from now on):

$$U = -\frac{1}{2} g^{-1} \int \overline{B_{\rho\rho} B} \, d\rho \tag{28b}$$

If one further introduces the spectrum of the eddy potential energy $U(k)$:

$$U = \int U(k) \, dk \tag{28c}$$

use of Eqs. (12a) with Λ in the lowest order and Eqs. (28b) and (28c) gives:

$$U(k) = -\frac{1}{2} (f r_d)^2 \int S_h(k) \bar{h}^{-1} \, d\rho, \quad S_h(k) = k \int \overline{h(\mathbf{k}) h^*(\mathbf{k}')} \, d^2\mathbf{k}' \, d\mathbf{n} \tag{28d}$$

Differentiating Eq. (28d) with respect to time, and since both $\bar{h}$ and r_d have very long characteristic time scales, one obtains:

$$\frac{\partial}{\partial t} S_h(k) = k \int Re\left[\overline{h_t(\mathbf{k}) h^*(\mathbf{k}')}\right] d^2\mathbf{k}' \, d\mathbf{n} \tag{28e}$$

Using the equation for h given by Eq. (10c), the first term in the rhs yields zero contribution; the last two terms express the transformation of energy within eddies that we discuss in Appendix B; therefore, the contribution of the second term of (10c) can only be interpreted as the contribution due to the interaction of large mean fields with the eddies. In Fig. 1, such process is labeled 1. The corresponding contribution to $\partial U(k)/\partial t$ must be interpreted as the effective rate of production of eddy potential energy (per unit horizontal area) and thus we have:

$$P_b = (f r_d)^2 \int (\mathbf{F}_h \cdot \nabla \bar{h}) \bar{h}^{-1} \, d\rho = (f r_d)^2 \int \mathbf{u}_* \cdot \nabla \bar{h} \, d\rho \tag{29}$$

We are in the position to compute K_t. Let us go back to (27b). Within our model, K is governed by the inverse kinetic energy cascade flux ε_k and by the eddy length scale $\ell \sim r_d$. Thus, only a Kolmogorov-type relation $K \sim (\varepsilon_\kappa \ell)^{2/3}$ is allowed. Notice, however that such a relation does not imply a Kolmogorov spectrum since ε_κ is not a constant but depends on the wavenumber k due the linear interaction of different isopycnal layers via the (linear) Bernoulli function B_0. Introducing (15d) and using (29) with (17), Eq. (27b) gives:

$$K_t^{1/2}[K_t - 6.7\eta\sigma_t^{1/2}\phi] = 0 \tag{30a}$$

which has two solutions:

$$K_t = 5.7\eta\phi, \quad K_t = 0 \tag{30b}$$

The function ϕ, with dimensions of a velocity square, does not depend on depth but on location through both r_d and f. It is given by

$$\phi = (\phi_1 + \phi_2)\phi_3^{-1} \tag{30c}$$

$$\phi_1 = -A_1 \int \Gamma^{1/2}[\bar{h}^{-1}\nabla\bar{h} - \langle \bar{h}^{-1}\nabla\bar{h}\rangle] \cdot \nabla\bar{h} \, d\rho \tag{30d}$$

$$\phi_2 = A_2 \int \Gamma^{1/2}(\mathbf{e} \times \nabla\bar{h}) \cdot (\bar{\mathbf{u}} - \langle\bar{\mathbf{u}}\rangle) \, d\rho \tag{30e}$$

$$\phi_3 \equiv \int \Gamma^{3/2}\bar{h} \, d\rho \tag{30f}$$

where $A \equiv r_d^4 f^2$ and $A_2 \equiv (1 + \sigma_t^{-1}) r_d^2 f$. Since $\phi(\Gamma)$ is a function of Γ, from Eq. (30b) it follows that so is K_t and from (25) we then have $a_0 = a_0(\Gamma)$. As a consequence, Eq. (24a) for $\Gamma(\rho)$ must be solved iteratively.

14. Predictions and tests of the model

14.1. Baroclinic nature of the bolus velocity

Using (17a,b,c) and (15d,e), it is easy to verify that $\mathbf{u}_*$ satisfies the relation:

$$\int \mathbf{u}_*(z)\,\mathrm{d}z = 0 \tag{31}$$

which shows that $\mathbf{u}_*$ is a baroclinic velocity, as expected. Previous models did not automatically satisfy (31) and additional delta functions were required at the surface so as to satisfy (31) (for a recent discussion, see Killworth, 2003).

14.2. Profile of eddy kinetic energy

Here we compare the predicted profile $\Gamma(\rho)$ with the measurements by Richardson (1983a) presented within the vertical section along 55°W in the interval 15°N–45°N. The maximum of the eddy kinetic energy occurs at 38°N (Gulf Stream). Using the latter data, we computed the normalized profile $\Gamma(z) = K(z)/K_\mathrm{t}$ and compared it with the model results Eqs. (24a), (25) and (17c). When using Eq. (25), we employed $K_\mathrm{t} = 0.2\ \mathrm{m^2\,s^{-2}}$ as from the same data. In addition, to compute r_d and Ψ in Eqs. (25) and (17c), we needed the profiles of $\bar{\mathbf{u}}(z)$, $N(z)$ and $\nabla\,\bar{h}$ which however are not given in Richardson (1983a). For this reason, we obtained this information from (Richardson, 1983b; Owens, 1984; Antonov et al., 1998; Boyer et al., 1998). The behavior predicted by the model is in good agreement with the measured profile by Richardson (1983a). An additional prediction of the present model is that the profile of the variable $\Gamma(z)/N(z)$ has two maxima at z_t and z_b and a minimum at $z \sim -1$ km. This is also in agreement with the measured values (Schmitz, 1994). Since the mesoscale diffusivity κ_M depends on $K^{1/2}(z)$ as Eq. (18) shows, the predicted behavior of $\kappa_\mathrm{M}(z)$ has the form qualitatively similar to that depicted in Fig. 2. When compared with Fig. 10a of Karsten and Marshall (2002), the behaviors are quite similar.

14.3. Mesoscale diffusivity

Using typical values of $K_\mathrm{t} \sim (0.5\text{–}1)10^{-2}\ \mathrm{m^2\,s^{-2}}$ (Stammer, 1998), and $r_\mathrm{d} \approx 30$ km, Eq. (18) gives:

$$\kappa_\mathrm{M}(\mathrm{surface}) \approx 3s^{1/2}10^3\ \mathrm{m^2\,s^{-1}} \tag{32a}$$

Since the filling factor $s < 1$, Eq. (32a) is close to the value used in the GM model (Gent and McWilliams, 1990; Gent et al., 1995). Karsten and Marshall (2002) used for κ_M (surface) the models of Holloway (1986) and Keffer and Holloway (1998) and the TOPEX/Poseidon data for the sea surface height. Their result, shown in their Fig. 2, is:

$$10^3 \leqslant \kappa_\mathrm{M}(\mathrm{surface}) < 3 \times 10^3\ \mathrm{m^2\,s^{-1}} \tag{32b}$$

which is in agreement with (32a). The function $\kappa_\mathrm{M}(z)$ is given by (18) and (30b):

$$\kappa_\mathrm{M}(\rho) = Cr_\mathrm{d}\phi^{1/2}\Gamma^{1/2}(\rho), \quad C = 4.3(s\eta)^{1/2} \tag{32c}$$

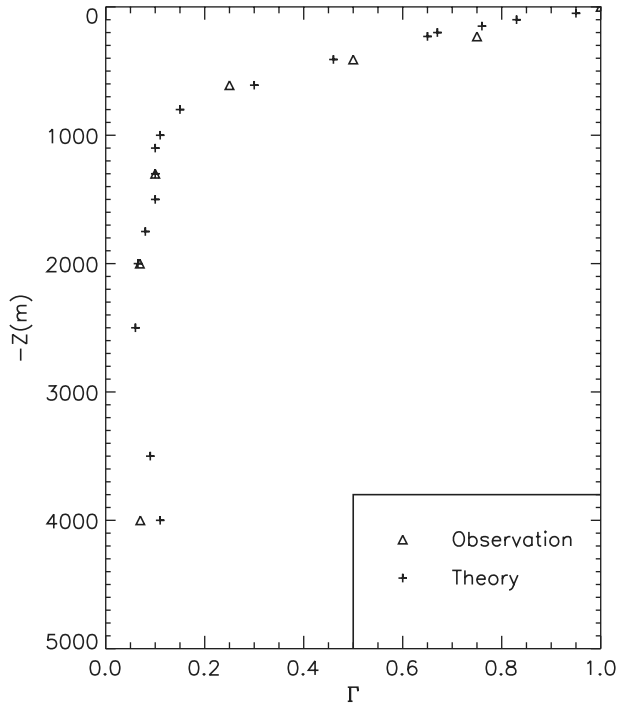

Fig. 2. Eddy kinetic energy profile $\Gamma(\rho)$ defined in Eq. (15d). Measured data for the Gulf Stream 39°N, 55°W (Richardson, 1983a) are represented by Δ while model results are represented by crosses (+).

Since r_d and ϕ do not depend on depth, the z-dependence of κ_M stems form $\Gamma(\rho)$ which we have plotted in Fig. 2. It follows that $\kappa_M(z)$ is predicted to be the largest at the top, followed by a rapid decrease, ultimately reaching a value constant with depth. This behavior is in accordance with the heuristic expressions suggested by Visbeck et al. (1997) and Karsten and Marshall (2002, Fig. 10). Using an eddy resolving code, Bryan et al. (1999) found that an overall consistent ocean model was obtained with:

$$\kappa_M(z) = 0.13 r_d^2 f Ri^{-1/2} \tag{32d}$$

A plot of $Ri^{-1/2}$ vs. z shows that $\kappa_M(z)$ has the same z-dependence as the one exhibited in Fig. 2. To compute $\kappa_M(z)$ from (32c), we need to compute ϕ from (30c)–(30f). Using an eddy resolving ocean code, we have done so and the result is:

$$\phi \sim 0.1 \text{ m}^2\,\text{s}^{-2} \tag{32e}$$

which yields:

$$\kappa_M(z) \sim C 10^3 \Gamma^{1/2}(z) \text{ m}^2\,\text{s}^{-1} \tag{32f}$$

which, at the surface, is quite close to (32a). In addition, the mesoscale kinetic energy K is estimated to be:

$$K \sim 10^{-2} \text{ m}^2\,\text{s}^{-2} \tag{32g}$$

which is also in agreement with measured data (Schmitz, 1996; Stammer, 1998).

14.4. Energy considerations

Substitution of (17a) and (17c) into (29) leads to the presence of two terms in P_b, namely:

$$P_b = P_b(1) + P_b(2) \tag{33a}$$

where

$$(fr_d)^{-2} P_b(1) = -\int \kappa_M [\bar{h}^{-1}\nabla\bar{h} - \langle \bar{h}^{-1}\nabla\bar{h}\rangle] \cdot \nabla\bar{h}\, d\rho \tag{33b}$$

$$P_b(2) = -f(1+\sigma_t^{-1}) \int \kappa_M \mathbf{e} \times [\bar{\mathbf{u}} - \langle \bar{\mathbf{u}}\rangle] \cdot \nabla\bar{h}\, d\rho \tag{33c}$$

In Appendix C we show that:

$$P_b(1) > 0, \quad P_b(2) < 0 \tag{33d}$$

which has the following physical interpretation. While the first two terms in the bolus velocity (17c) correspond to the extraction of energy by the mesoscales from the mean field $\bar{h}$, the last two terms, which contribute a negative P_b, correspond to the back-scatter of a fraction of the mesoscale potential energy to the mean field $\bar{h}$. It is important to stress that the presence of $P_b(2)$ is not due to dissipation at the smallest scales (an irreversible process) since it is still within the adiabatic approximation and it is a reversible process since that energy is put back into the large scales reservoir of energy.

14.5. Energy dissipation rate

Using Eqs. (24a) $K = K_t \Gamma$ and Eq. (30b) in $K \sim (\varepsilon r_d)^{2/3}$, we obtain:

$$\varepsilon \sim (\varphi\Gamma)^{3/2} r_d^{-1} \sim 10^{-10}\ \mathrm{m^2\,s^{-3}} \tag{33e}$$

a value which is in agreement with the values of Toole et al. (1994, Table 1).

14.6. The dissipation length scale ℓ_1

As discussed in Appendix B, ℓ_1 is determined from the condition that the turbulent time scale $\varepsilon^{-1/3}\ell_1^{2/3}$ be of the order of the Coriolis time scale f^{-1}. Combining this relation with $K \sim (\varepsilon r_d)^{2/3}$, we obtain:

$$\ell_1 \sim K^{3/4} r_d^{-1/2} f^{-3/2} \sim 1\ \mathrm{km} \tag{33f}$$

14.7. Geostrophic turbulence

To understand the relation between the energy cycle described in Appendix B and Charney's (1971) geostrophic turbulence, we begin with the definition of PV (potental vorticity) given in the

first of (1h). Separating ζ and h into their mean and fluctuating components, we have to the first-order in the fluctuating fields:

$$\bar{h}q' = \zeta' - f\bar{h}^{-1}h' \tag{33g}$$

Using the geostrophic approximation to evaluate ζ' and using Eqs. (4c,d) to compute the second term, Eq. (33g) becomes:

$$\bar{h}q' = (f\bar{\rho})^{-1}\nabla^2 B' - f(\bar{h}g)^{-1}B'_{\rho\rho} \tag{33h}$$

Once transformed to z-coordinates, the rhs of Eq. (33h) coincides (without the β term) with the fluctuating component of the *pseudo-potental vorticity* in Charney's Eq. (8). Let us consider Eq. (33h) at the two scales, r_d and ℓ_1 discussed in Appendix B. In the first case, use of Eqs. (11a)–(11c) shows that both terms in (33h) are of the same order which means that the first term (relative vorticity) does not dominate and thus is not conserved by itself. In turn, this implies that there is no enstrophy cascade but only inverse energy cascade (energy is conserved). As one moves to smaller scales (larger wavenumbers), the first term becomes dominant and so does relative vorticity which makes enstrophy cascade possible, provided there is a feeding mechanism. The transformation of potential energy into kinetic energy at ℓ_1 (Appendix B) also generates enstrophy. Beginning at $k_1 \sim \ell_1^{-1}$, energy cascades upscale to smaller wavenumbers while enstrophy cascades downscale to larger k's. Thus, for $k > \ell_1^{-1}$, Charney's energy spectrum k^{-3} is realized.

These predictions are confirmed by measurements of Samelson and Paulson (1988, SP) whose most statistically representative data are shown in their Fig. 8 corresponding to the spectrum of horizontal temperature gradient vs. horizontal wavenumbers. (the eddy potential energy spectrum is obtained by multiplying by k^{-2}). In SP Fig. 8, the flat range of $U(k)$ begins at $k_0 \approx 3\ 10^{-2}$ rad/km (SP employ cycles/km) which coincides with the prediction of the present model: k_0 is given by Eq. (13b) and with the value of r_d of 40 km determined by SP, the predicted k_0 coincides with that of SP. Furthermore, the spectrum $U(k) \sim k^{-3}$ begins at $k_1 \approx 1$ rad/km also in agreement with the model prediction (33f) that $k_1 = 1/\ell_1 \sim 1$ rad/km. Finally, in the region $k_0 < k < k_1$, the spectrum of $U(k)$ given in Fig. 8 of SP exhibits a power law spectrum less steep than −3 and much closer to a Kolmogorov −5/3 predicted by our model.

15. Complete model

From a practical viewpoint, it may be of interest to have the model equations in isopycnal coordinates collected together. This is done in Appendix D.

16. Conclusions

The primary goal of the work was to derive an expression for the three mesoscale terms that enter the coarse resolution ocean model equations. They are the thickness flux, the relative vorticity flux and the mesoscale kinetic energy K, Eq. (1m). We have derived three analytic

expressions, Eqs. (17), (18), (21), (24a) and (30) by solving the eigenvalue problem for the Bernoulli function, Eq. (11a). To arrive at this equation, we have used the following ingredients:

(1) the non-linear interactions are treated with a turbulence model that was previously tested on a variety of flows,
(2) the mesoscale eddy field are low frequency $\omega < f$,
(3) the characteristic length scale of the large scale fields considerably exceeds that of the mesoscale eddies,
(4) $|\bar{\mathbf{u}}/\mathbf{u}'| < 1$. Even though this ratio is not very small, corrections to all results enter as the square of it, namely they are of the order of MKE/EKE ~ 0.1.
(5) we have assumed that the largest contribution to the mesoscale fluxes and EKE comes from the region in wavenumber space where the spectra have their maxima and that all spectra have approximately the same width.

The results we have obtained can be summarized as follows:

(1) The form of the bolus velocity $\mathbf{u}_*$ given by Eqs. (17a)–(17c) does not coincide with either of the two most frequently used expressions, Eq. (2a) and (2b). The latter are part of more general expressions.
(2) *The additional terms* that appear in the bolus velocity $\mathbf{u}_*$ have a structure similar to that described by Bryan et al. (1999), namely that: "the bolus velocity is more than just an agent of thickness mixing and flows are set up that are not closely linked to thickness source or sinks". In fact, the new terms depend on the difference between the mean flow mean velocity $\bar{\mathbf{u}}$ and its average $\langle\bar{\mathbf{u}}\rangle$.
(3) There are no a priori reasons why the extraction of energy from the large scales ought to be 100% efficient. Even within the adiabatic approximation, some of the mesoscales energy can be back-scattered to the large scale field, reducing the efficiency of the "flattening of the isopycnals" process and restoring some of the mean potential energy. The process is due to the presence of additional terms in the expression for $\mathbf{u}_*$.
(4) The bolus velocity $\mathbf{u}_*$ satisfies the baroclinicity condition Eq. (19).
(5) While several studies have strived to relate the mesoscale diffusivity κ_M to the large scale resolved fields, less attention has been paid to the fact that within a strictly adiabatic model, κ_M is actually infinite. This is due to the fact that without irreversible processes such as dissipation (which by definition is absent in the adiabatic limit), the energy drawn by the eddies would keep on increasing, ultimately leading to infinite potential and kinetic energy. Since $\kappa_M \sim r_d K^{1/2}$, Eq. (18), this leads to an infinity diffusivity. The present model includes dissipation and shows that $K \sim \eta$, where η can be viewed as the degree of adiabaticity, the limit $\eta \to \infty$ representing full adiabaticity.
(6) The mesoscale diffusivity κ_M given by Eq. (18) is no longer an adjustable parameter since it can now be computed in terms of the resolved fields. The predicted z-dependence of κ_M is in agreement with the one suggested by heuristic models.
(7) The mesoscales affect the mean momentum equations via the relative vorticity flux $\mathbf{F}_\zeta$. The present model yields expression (21) for $\mathbf{F}_\zeta$. It contains both a gradient of the mean potential vorticity and the difference $\bar{\mathbf{u}} - \langle\bar{\mathbf{u}}\rangle$.

(8) The relative vorticity flux, the PV-flux and the thickness flux are related:

$$\mathbf{F}_q = \mathbf{F}_\zeta - \hat{q}\mathbf{F}_\mathrm{h} = \mathbf{F}_\zeta - \hat{q}\bar{h}\mathbf{u}_* \tag{34a}$$

From this, one derives that the PV-flux has the form:

$$\mathbf{F}_q = -\bar{h}\kappa_\mathrm{M}\nabla\hat{q} + \mathbf{F}_q^* \tag{34b}$$

where

$$\mathbf{F}_q^* = \mathbf{F}_\zeta - \hat{q}\bar{h}(\text{Additional terms}) \tag{34c}$$

where Eq. (2d) must be used. The RHY-model (Rhines and Holland, 1979; Rhines and Young, 1982a,b) showed that the q-flux "should have a down-gradient component". The first term in Eq. (34b) confirms that conclusion but in addition it provides the explicit form of the extra terms that the RHY model could not compute since it did not provide a closure.

(9) The model shows that the relative vorticity $\mathbf{F}_\zeta$ is *entirely contributed by the ageostrophic component* of the mesoscale velocity field. Thus, if one assumes a geostrophic flow, Eq. (34a) reduces to:

$$\mathbf{F}_q = -\hat{q}\mathbf{F}_\mathrm{h} \tag{34d}$$

in which case there would be only one flux to be modeled, in addition to the eddy kinetic energy K. However, as shown in Appendix B, the ageostrophic mesoscale velocity is instrumental in closing the Lorenz energy clycle.

(10) At the present stage of development of the model, we are unable to compute the filling factor s in Eqs. (18) and the adiabaticity index η, Eq. (30b). The reasons are strictly technical. Had we solved the mesoscale dynamic equations numerically rather than analytically, we would have obtained the spectra in k-space and with that information we could have computed s and η. For the time being, we chose to solve the equations analytically to exhibit the major features in a way than can be interpreted physically. In reality, even if we don't know the numerical values of s and η, they have a well-defined physical meaning and are not fudge factors. Future work on this problem should be able to compute them.

In conclusion, we believe that a sufficient numbers of new results have emerged from this analysis to justify testing the new mesoscale model with an eddy resolving ocean code and, if successful, with a coarse resolution code.

Acknowledgements

VMC would like to thank Drs. P. Killworth, T. McDougall and D.P. Marshall for suggestions that helped improve the original manuscript. Special thanks are due to Dr. R.J. Greatbatch for a very instructive exchange of ideas about the mean momentum equations. The authors would like to thank the NASA Climate Program and the NASA Oceanography Program managed by T. Lee and E. Lindstrom for financial support. MSD would like to thank the Physical Oceanography Division of NSF for partial financial support (NSF OCE-0241668).

Appendix A. Bolus velocity

We begin by writing Eq. (16a) as

$$\mathbf{F}_{\mathrm{h}} = \int \widetilde{\mathbf{F}}_{\mathrm{h}}(\mathbf{k})\, \mathrm{d}^2\mathbf{k} \tag{A.1a}$$

where

$$\mathbf{F}_{\mathrm{h}}(\mathbf{k})\delta(\mathbf{k}-\mathbf{k}') = Re\overline{h'(\mathbf{k})\mathbf{u}^*(\mathbf{k}')} = -(\mathbf{e}\times\mathbf{n})Re\overline{\bar{h}'(\mathbf{k})u^*(\mathbf{k}')} \tag{A.1b}$$

Combining (11a), (12a) and (10a,d) we obtain:

$$Re\overline{h'(\mathbf{k})\mathbf{u}^*(k')} = -\sigma_{\mathrm{t}}\Omega_{\mathrm{r}}\tau k_0\bar{h}f^{-1}\overline{u(\mathbf{k})u^*(\mathbf{k}')} \tag{A.1c}$$

where Ω_{r} is the real part of Ω. Since the field $u(\mathbf{k})$ is axisymmetric, the correlation function in the right hand side of (A.1c) is related to the energy spectrum $E(k)$:

$$\overline{u(\mathbf{k})u^*(\mathbf{k}')} = (\pi k)^{-1}E(k)\delta(\mathbf{k}-\mathbf{k}') \tag{A.1d}$$

and thus:

$$Re\overline{h'(\mathbf{k})u^*(\mathbf{k}')} = -\sigma_{\mathrm{t}}f^{-1}\pi^{-1}E(k)\Omega_{\mathrm{r}}\tau\bar{h}\delta(\mathbf{k}-\mathbf{k}') \tag{A.1e}$$

Substituting back into (A.1a) and (A.1b) and using (12b), we obtain Eq. (16b) and (16c) of the text where we also employ the relation:

$$(2\pi)^{-1}\int(\mathbf{e}\times\mathbf{n})(\mathbf{A}\cdot\mathbf{n})\,\mathrm{d}n = \frac{1}{2}\mathbf{e}\times\mathbf{A} \tag{A.1f}$$

Appendix B. Energy cycle

Because of the earth's rotation, the large-scale mean velocity is perpendicular to the gradient of the mean potential energy and the latter performs no work. As a result, mean potential energy is two orders of magnitude larger than the mean kinetic energy (Riley and Lelong, 2000). Since mean potential energy, whose rate of production we denote by P_{b} (with the subscript b for baroclinic), cannot feed directly turbulent kinetic energy, it feeds eddy potential energy (process 1, Fig. 1). The process can be identified directly in Eq. (10c). The last term represents the "cascade of the thickness variance" which we denote by ε_{p}. The penultimate term in the rhs of (10c) describes the energy exchange between the fields u_{s} and h via the ageostrophic velocity field u_{p}. In fact, this term performs positive work on the field h (process 6). This work is almost fully balanced by the negative work of the last term (process 2). An analogous balance occurs in the equation for the field u_{s}, Eq. (5a). The last term, represented by ε_{κ}, performs positive work on the field u_{s} (process 4). This work is balanced by the negative work of the fu_{p} term (process 5). This analysis implies that near $k \sim k_0$ *the ageostrophic eddy field* u_{p} *almost fully transforms the geostrophic velocity fluctuations field into thickness fluctuations* (*processes 5,6*). The field h in turn propagates in k-space to higher k's until k_1 where the turbulent time scale becomes of the order of the Coriolis time scale f^{-1}. A typical value is $\ell \sim 1$ km; it is important to note that at k_1, vertical shear fluctuations are

the largest and are of the order of the large scale Brunt–Vaisala frequency, N. Stated differently, the Richardson number $Ri \leqslant 1$ thus enabling shear fluctuations to generate vertical turbulence. *One can thus view ℓ_1 as the horizontal scale associated with vertical turbulence*. This result confirms the model by Gargett (1993) whereby vertical turbulence is generated by the fluctuations of shear. In summary, the energy cycle operates as follows:

1. at scales $\sim r_d$, the gradient $\nabla\bar{h}$ of the large scale mean thickness (baroclinic instability) which is related to the mean potential energy, feeds the thickness variance which is related to the eddy's potential energy,
2. the latter then cascades from large to small scales (process 2),
3. at ℓ_1, a fraction of eddy potential energy transforms into eddy kinetic energy (process 3a) while the remaining eddy potential energy generates diapycnal turbulence whose energy is dissipated into heat (process 3b),
4. the determination of ℓ_1 follows from the condition that the corresponding turbulent time scale is of the order of the Coriolis time scale f^{-1}. A typical value is $\ell_1 \sim 1$ km,
5. beginning at ℓ_1, eddy kinetic energy cascades backward to r_d (process 4) where it reverts back to eddy potential energy, which is also continuously fed by the baroclinic instabilities.

Appendix C. The integrals in Eqs. (30a)–(30f)

Here, we study the two integrals:

$$I_1 = -\int \kappa_M \left[\bar{h}^{-1}\nabla\bar{h} - \langle\bar{h}^{-1}\nabla\bar{h}\rangle\right]\cdot\nabla\bar{h}\,d\rho \tag{C.1}$$

$$I_2 = -\int \kappa_M \mathbf{e}\times(\bar{\mathbf{u}} - \langle\bar{\mathbf{u}}\rangle)\cdot\nabla\bar{h}\,d\rho \tag{C.2}$$

that appear in the equation for the rate of production of eddy potential energy P_b, Eqs. 30d,30e. Using Eq. (18) and the definition of the weighted average $\langle\cdot\cdot\rangle$ given in Eqs. (15d), we obtain from (C.1) (to simplify notation, we don't write the upper and lower limits of integrations which are z_t and z_b):

$$I_1 = 1.8 r_d K_t^{1/2}\int \Gamma^{1/2}(z)\left[\bar{h}^{-1}\nabla\bar{h} - \langle\bar{h}^{-1}\nabla\bar{h}\rangle\right]^2 dz \tag{C.3}$$

which is clearly positive. Using (15c), we rewrite (C.2) as:

$$I_2 = \int \kappa_M(\mathbf{e}\times\bar{\mathbf{u}})\cdot\left[\bar{h}^{-1}\nabla\bar{h} - \langle\bar{h}^{-1}\nabla\bar{h}\rangle\right]dz \tag{C.4}$$

To ascertain the sign of this integral, we need to evaluate the vertical scales of the functions in the integrand. Since $\kappa_M \sim K^{1/2}(z)$, the variations of κ_M occur on scales $\geqslant 10^3$ m, as is clear from Fig. 1. The same vertical scale characterizes the term $\bar{h}^{-1}\nabla\bar{h}$. In fact:

$$\int \bar{h}^{-1}\nabla\bar{h}\,dz = -\int \nabla z_\rho\,d\rho = \nabla(\bar{z}_{top} - \bar{z}_{bot}) \sim 10^{-3} \tag{C.5}$$

while near the surface, $\bar{h}^{-1}\nabla\bar{h} \sim 10^{-6}$ m^{-1}. Thus, the vertical scale of this function is $\sim 10^3$ m. As for the function $\bar{\mathbf{u}}(z)$, its characteristic scale is $|\bar{\mathbf{u}}/\bar{\mathbf{u}}_z| \sim 10^2$ m. In fact, $|\bar{\mathbf{u}}| \sim 10^{-2}$ m s^{-1} whereas

$$|\bar{\mathbf{u}}_z| \sim Ri^{-1/2}N^{-1} \sim 10^{-4}s^{-1} \tag{C.6}$$

since $Ri \sim 10^3$ and $N^2 \sim 10^{-5}s^{-2}$. Therefore, the integral (C.4) is contributed mostly by the upper layer of the thickness (few hundred meters), a scale that is considerably smaller than the characteristic vertical scale of $\bar{h}^{-1}\nabla_\sigma\bar{h}$ which is $\geqslant 10^3$ m. For this reason, the first term exceeds the second term. Integrating by parts, using the geostrophic relation and the boundary conditions on B, we obtain:

$$gfI_2 = \int \kappa_{\mathrm{M}}\nabla B\cdot\nabla B_{\rho\rho}\,\mathrm{d}\rho = -\int \kappa_{\mathrm{M}}(\nabla B_\rho)^2\,\mathrm{d}\rho - \int(\partial_\rho\kappa_{\mathrm{M}})\nabla B\cdot\nabla B_\rho\,\mathrm{d}\rho \tag{C.7}$$

Since the vertical scale of ∇B coincides with that of $\bar{\mathbf{u}}$, the first term, which is negative, dominates.

Appendix D. Complete model in isopycnal coordinates

Dynamic equation for the mean thickness $\bar{h}$:

$$\frac{\partial}{\partial t}\bar{h} + \nabla\cdot(\overline{h\mathbf{u}} + \mathbf{F}_{\mathrm{h}}) = 0 \tag{D.1}$$

Mesoscale flux:

$$\mathbf{F}_{\mathrm{h}} = \bar{h}\mathbf{u}_* \tag{D.2}$$

Bolus velocity:

$$\mathbf{u}_* = -\kappa_{\mathrm{M}}\boldsymbol{\Psi} \tag{D.3}$$

$$\boldsymbol{\Psi} = -\hat{q}^{-1}\nabla\hat{q} + \langle\hat{q}^{-1}\nabla\hat{q}\rangle + (1+\sigma_{\mathrm{t}}^{-1})r_{\mathrm{d}}^{-2}f^{-1}\mathbf{e}\times(\bar{\mathbf{u}} - \langle\bar{\mathbf{u}}\rangle) \tag{D.4}$$

$$\boldsymbol{\Psi} = \bar{h}^{-1}\nabla\bar{h} - \langle\bar{h}^{-1}\nabla\bar{h}\rangle + (1+\sigma_{\mathrm{t}}^{-1})r_{\mathrm{d}}^{-2}f^{-1}\mathbf{e}\times(\bar{\mathbf{u}} - \langle\bar{\mathbf{u}}\rangle) \tag{D.5}$$

Vertical average:

$$\langle X\rangle \equiv \int X\Gamma^{1/2}\bar{h}\,\mathrm{d}\rho\left(\int \Gamma^{1/2}\bar{h}\,\mathrm{d}\rho\right)^{-1} \tag{D.6a}$$

$$\Gamma(\rho) \equiv K(\rho)/K_{\mathrm{t}} \tag{D.6b}$$

The lower and upper limits in the integral in (D.6a) are ρ_{t} and ρ_{b}.

Mesoscale diffusivity:

$$\kappa_{\mathrm{M}} = 1.8s^{1/2}r_{\mathrm{d}}K_{\mathrm{t}}^{1/2}\Gamma^{1/2}(\rho) \tag{D.7}$$

$$\Gamma(\rho) = \frac{|B_1|^2 + |a_0^2|}{1+|a_0|^2} \tag{D.8}$$

The function B_1 is solution of eigenvalue problem:

$$\left(\frac{\partial^2}{\partial\rho^2} + \lambda_n^2\right)B_n = 0 \tag{D.9a}$$

where

$$\lambda_n = (r_n f)^{-1} N \bar{h} \tag{D.9b}$$

with $r_1 \equiv r_d$. The boundary conditions are (the indices t and b stand for top and bottom):

$$\frac{\partial}{\partial \rho} B_n(\rho) = 0 \quad \text{at } \rho = \rho_{t,b} \tag{D.9c}$$

and B_1 is normalized such that:

$$B_1(\rho_t) = 1 \tag{D.9d}$$

Furthermore:

$$|a_0|^2 = 2 f^2 r_d^4 K_t^{-1} \mathbf{J}^2 \tag{D.10}$$

$$\mathbf{J} = H^{-1} \int \theta(\rho_* - \rho) \mathbf{\Psi} \bar{h} \, d\rho \tag{D.11}$$

and $\theta(x) = \pm 1$ for $x > 0$ and $x < 0$. The lower/upper limits in the integral in (D.11) are ρ_t and ρ_b.

Surface kinetic energy K_t:

$$K_t = 5.7 \eta \phi \tag{D.12}$$

$$\phi = (\phi_1 + \phi_2) \phi_3^{-1} \tag{D.13}$$

$$\phi_1 = -A_1 \int |B_1| [\bar{h}^{-1} \nabla \bar{h} - \langle \bar{h}^{-1} \nabla \bar{h} \rangle] \nabla \bar{h} \, d\rho \tag{D.14}$$

$$\phi_2 = A_2 \int |B_1| (\mathbf{e} \times \nabla \bar{h}) \cdot (\bar{\mathbf{u}} - \langle \bar{\mathbf{u}} \rangle) \, d\rho \tag{D.15}$$

$$\phi_3 \equiv \int |B_1|^3 \bar{h} \, d\rho \tag{D.16}$$

$$A_1 \equiv r_d^4 f^2, \quad A_2 \equiv (1 + \sigma_t^{-1}) r_d^2 f \tag{D.17}$$

The value of σ_t is 0.72 (CD96).

Dynamic equation for the mean velocity $\bar{\mathbf{u}}$:

$$\bar{\mathbf{u}}_t + (f + \bar{\zeta}) \mathbf{e} \times \bar{\mathbf{u}} = -\nabla_{\bar{B}_*} - \mathbf{e} \times \mathbf{F}_\zeta \tag{D.18a}$$

where

$$\bar{B}_* = \frac{1}{2} \bar{\mathbf{u}}^2 + K + \rho_0^{-1} (\bar{p} + g \bar{\rho} z) \tag{D.18b}$$

Relative vorticity flux:

$$\mathbf{F}_\zeta = K (1 + \sigma_t)^{-1} \mathbf{e} x \langle \hat{q}^{-1} \nabla \hat{q} \rangle - K (\sigma_t r_d^2 f)^{-1} (\bar{\mathbf{u}} - \langle \bar{\mathbf{u}} \rangle + \mathbf{c}_R) \tag{D.19a}$$

$$\mathbf{c}_R = \sigma_t r_d^2 \mathbf{e} \times \nabla f \tag{D.19b}$$

References

Andrews, D.G., McIntyre, M.E., 1976. Planetary waves in horizontal and vertical shear the generalized Eliassen–Palm relation and the mean zonal acceleration. J. Atmos. Sci. 33 (11), 2031–2053.

Andrews, D.G., McIntyre, M.E., 1978. An exact theory of non-linear waves on a Lagrangian mean flow. J. Fluid Mech. 89, 609–646.

Andrews, D.G., Holton, J.R., Leovy, C.B., 1987. Middle Atmosphere Dynamics. Academic press. 489pp.

Antonov, J., Levitus, S., Boyer, T.P., Conkright, M., O'Brein, T., Stephens, C., 1998. World Ocean Atlas, Vol.1: Temperature of the Atlantic Ocean, NOAA Atlas NESDIS 27, US Government Printing Office, Washington, DC, 166pp.

Boyer, T.P., Levitus, S., Antonov, J., Conkright, M., O'Brein, T., Stephens, C., 1998. World Ocean Atlas, Vol. 4: Salinity of the Atlantic Ocean, NOAA Atlas NESDIS 30, US Government Printing Office, Washington, DC, 166pp.

Bryan, K., Dukowicz, J.K., Smith, R.D., 1999. On the mixing coefficient in the parameterization of bolus velocity. J. Phys. Ocean. 29, 2442–2456.

Canuto, V.M., Dubovikov, M.S., 1996a. A dynamical model for turbulence: I. General formalism. Phys. Fluids 8, 571–586.

Canuto, V.M., Dubovikov, M.S., 1996b. A dynamical model for turbulence: II. Shear driven flows. Phys. Fluids 8, 587–598.

Canuto, V.M., Dubovikov, M.S., 1996c. A dynamical model for turbulence: III. Numerical results. Phys. Fluids 8, 599 (with A. Dienstfrey).

Charney, J.E., 1971. Geostrophic turbulence. J. Atmos. Sci. 28, 1087–1095.

Ciliberto, S., Cioni, S., Laroche, C., 1996. Large scale flow properties of turbulent thermal convection. Phys. Rev. E 54, 5901.

Danabasoglu, G., McWilliams, J.C., Gent, P.R., 1994. The role of mesoscale tracer transports in global ocean circulation. Science 264, 1123–1126.

Drijfhout, S.S., Hazeleger, W., 2001. Eddy mixing of potential vorticity vs. thickness in an isopycnal ocean model. J. Phys. Ocean. 31, 481–505.

Dukowicz, J.K., Greatbatch, R.J., 1999. The bolus velocity in the stochastic theory of ocean turbulent tracer transport. J. Phys. Ocean. 29, 2232–2239.

Gargett, A., 1993. Parameterizing the effect of small scale mixing in large scale numerical models. In: Modeling Oceanic Climate Interactions NATO ASI Series, vol. 1, 11. Springer-Verlag, New York, pp. 185–204.

Geller, M.A., Nash, E.R., Wu, M.-F., Rosenfeld, J.E., 1992. Residual circulations calculated from satellite data. Their relations to observed temperature and ozone distributions. J. Atoms. Sci. 49, 1127–1137.

Gent, P.R., McWilliams, J.C., 1990. Isopycnal mixing in ocean circulation models. J. Phys. Ocean. 20, 150–155.

Gent, P.R., Willebrand, J., McDougall, T., McWilliams, J.C., 1995. Parameterizing eddy induced tracer transports in ocean circulation models. J. Phys. Ocean. 25, 463–474.

Gille, S.T., Davis, R., 1999. The influence of mesoscale eddies on coarsely resolving density: an examination of subgrid-scale parameterization. J. Phys. Ocean. 29, 1109–1123.

Greatbatch, R.J., 1998. Exploring the relationship between eddy-induced transport velocity, vertical momentum transfer and the ispycnal flux of potential vorticity. J. Phys. Ocean. 28, 422–432.

Greatbatch, R.J., 2001. A framework for mesoscale eddy prameterization based on density-weighted averaging at fixed height. J. Phys. Ocean. 31, 2797–2806.

Greatbatch, R.J., McDougall, T.J., 2003. The non-boussinesq temporal residual mean. J. Phys. Ocean. 33, 1231–1239.

Griffies, S.M., Binning, C., Bryan, F.O., Chassignet, E.P., Gerdes, R., Hasumi, H., Hirst, A., Treguier, A.M., Webb, D., 2000. Developments in ocean modeling. Ocean Modell. 2 (3–4), 123–192.

Held, I.M., Larichev, V.D., 1996. A scaling theory for horizontally homogeneous, baroclinically unstable flow on a beta plane. J. Atmos. Sci. 53, 946–952.

Holland, W.R., Keffer, T., Rhines, P.B., 1984. Dynamics of the ocean general circulation: the potential vorticity field. Nature 308, 698–705.

Holloway, G., 1986. Estimation of oceanic eddy transport from satellite altimetry. Nature 323, 243–244.

Holton, J.R., 1992. An Introduction to Dynamic Meteorology. Academic Press, San Diego. 511p.

Karsten, R.H., Marshall, J., 2002. Constructing the residual circulation of the ACC from observations. J. Phys. Ocean. 32, 3315–3327.
Keffer, T., Holloway, G., 1998. Estimating Southern Ocean eddy flux of heat and salt from satellite altimetry. Nature 332, 624–626.
Killworth, P.D., 1997. On parameterization of eddy transport. J. Mar. Res. 55, 1171–1197.
Killworth, P.D., 2003. On the parameterisation of eddies in ocean models. XXIII IUGG, General Assembly, Sapporo, Japan, June 30–July 11.
Lee, M.M., Marshall, D.P., Williams, R.G., 1997. On the eddy transfer of tracers: advective or diffusive? J. Mar. Res. 55, 483–505.
McDougall, T.J., McIntosh, P.C., 1996. The temporal-residual-mean velocity. Part I: Derivation and scalar conservation equations. J. Phys. Ocean. 26, 2653–2665.
McDougall, T.J., Hirst, A.C., England, M.H., McIntosh, P.C., 1996. Implications of a new eddy parameterization for ocean models. Geophys. Res. Lett. 23, 2085–2088.
McDougall, T.J., McIntosh, P.C., 2001. The temporal-residual-mean velocity. Part II: Isopycnal interpretation and tracer and momentum equations. J. Phys. Ocean. 31, 1222–1246.
Medvedev, A., Greatbatch, R.J., 2003. On transport and mixing in the mesosphere and lower atmosphere: the role of rotational and diffusive fluxes. J. Gephys. Res., in press.
Nakamura, M., Chao, Y., 2000. On the eddy isopycnal thickness diffusivity of the Gent McWilliams subgrid mixing parameterization. J. Climate 13, 502–510.
Owens, W.B., 1984. A synoptic and statistical description of the Gulf Stream and subtropical gyre using SOFAR floats. J. Phys. Ocean. 14, 104–113.
Plumb, R.A., Mahlman, J.D., 1987. The zonally averaged transport characteristics of the GFDL general circulation model. J. Atmos. Sci. 44, 298–372.
Rhines, P.R., Holland, W.R., 1979. A theoretical discussion of eddy-driven mean flows. Dyn. Atmos. Ocean 3, 289–325.
Rhines, P.B., 1982. Basic dynamics of the large-scale geostrophic circulation. In: Summer Study Program in Geophysical Fluid Dynamics. Woods Hole Oceanographic Institution. p. 147.
Rhines, P.B., Young, W.R., 1982a. A theory of wind-driven ocean circulation. 1 Mid Ocean gyres. J. Mar. Res. 40 (Suppl.), 559–596.
Rhines, P.B., Young, W.R., 1982b. Homogenization of potential vorticity in planetary gyres. J. Fluid Mech. 122, 347–367.
Richardson, P.L., 1983a. A vertical section of eddy kinetic energy through the Gulf Stream system. J. Geophys. Res. 88, 2705–2709.
Richardson, P.L., 1983b. Eddy kinetic energy in the North Atlantic from surface drifters. J. Geophys. Res. 88, 4355–4367.
Riley, J.J., Lelong, M.P., 2000. Fluid motions in the presence of strong stable stratification. Ann. Rev. Fluid Mech. 32, 613–657.
Rix, N.H., Willenbrand, J., 1996. Parameterization of mesoscale eddies as inferred from high-resolution circulation models. J. Phys. Ocean. 26, 2281–2285.
Roberts, M.J., Marshall, D.P., 2000. On the validity of downgradient eddy closures in ocean models. J. Geophys. Res. 105, 28613–28627.
Samelson, R.M., Paulson, C.P., 1988. Towed thermistor chain observations of fronts in the subtropical North Pacific. J. Geophys. Res. 93, 2237–2246.
Schmitz Jr., W.J., 1994. Observation of vertical structure of the eddy field in the Kuroshio extension. J. Geophys. Res. 89, 6355–6364.
Schmitz Jr., W.J., 1996. The world ocean circulation. Vols. I and II, Woods Hole Oceanographic Institution, Woods Hole, Mass, 02543, WHOI-96-08.
Smith, R.D., 1999. The primitive equations in the stochastic theory of adiabatic stratified turbulence. J. Phys. Ocean. 29, 1865–1880.
Solovev, M., Stone, P.H., Malanotte–Rizzoli, P., 2002. Assessment of mesoscale eddy parameterizations for a single basin course resolution ocean model. J. Geophys. Res. 107 (C9), 1–19.

Stammer, D., 1997. Global characteristics of ocean variability estimated from regional TOPEX/POSEIDON altimeter measurements. J. Phys. Ocean. 27, 1743–1769.

Stammer, D., 1998. On eddy characteristics, eddy transport and mean flow properties. J. Phys. Ocean. 28, 727–739.

Toole, J.M., Polzin, K.L., Schmitt, R.W., 1994. Estimates of diapycnal mixing in the Abyssal ocean. Science 264, 1120–1123.

Treguier, A.M., Held, I.M., Larichev, V.D., 1997. On the parameterization of quasi geostrophic eddies in primitive equation ocean models. J. Phys. Ocean. 27, 567–584.

Treguier, A.M., 1999. Evaluating eddy mixing coefficients from eddy resolving ocean models: a case study. J. Mar. Res. 57, 89–108.

Tung, K.K., 1986. Nongeostrophic theory of zonally averaged circulation. Part I: Formulation. J. Atmos. Sci. 43, 2600–2618.

Visbeck, M.J., Marshall, J., Haine, T., Spall, M., 1997. On the specification of eddy transfer coefficients in coarse resolution ocean circulation models. J. Phys. Ocean. 27, 381–402.

Wardle, R., Marshall, J., 2000. Representation of eddies in primitive equation models by a PV flux. J. Phys. Oceanogr. 30, 2481–2503.

Wu, X.Z., Libchaber, A., 1992. Scaling relations in thermal turbulence. The aspect ratio dependence. Phys. Rev. A 45, 842.